Accurate and Efficient 2D Modelling of Historical Masonry Buildings Subjected to Settlements in Comparison to 3D Approaches

Alfonso Prosperi[1(✉)], Michele Longo[1], Paul A. Korswagen[1], Mandy Korff[1,2], and Jan G. Rots[1]

[1] Faculty of Civil Engineering and Geosciences, Delft University of Technology, Stevinweg 1, 2628 Delft, The Netherlands
a.prosperi@tudelft.nl

[2] Deltares, P.O BOX, 177, 2600 MH Delft, The Netherlands

Abstract. This paper presents an improved 2D modelling strategy which aims to represent the behavior of historical unreinforced masonry buildings on shallow foundations subjected to ground settlements. The application is presented with reference to a two-storey building, typical of the Dutch built heritage. The novelty comprises the inclusion of the effect of the lateral house-to-house separation walls of such old buildings. Additionally, the masonry strip foundation is modelled and supported by a boundary interface representing the interaction between the soil and the foundation. Two realistic hogging and sagging settlement configurations are applied to the model and their intensity is characterized using the angular distortion of the settlement shape. The response in terms of damage and deformations of the proposed modelling strategy is compared with the ones of five selected approaches based on the state of the art. For all the selected models, the damage severity is quantified objectively by means of a scalar parameter, which is computed considering the cracks' number, length, and width.

The results of the proposed 2D model agree in terms of displacements, crack patterns and damage with the 3D models. On the contrary, the façade models that do not include the effect of the lateral walls do not exhibit the same cracking and damage, resulting in lower damage and deformations for the same applied angular distortion. Accordingly, the proposed modelling strategy requires less modelling complexity and the analyses are 9 to 28 times faster to run with respect to the 3D models. The efficient and accurate model allows performing a wide number of analyses to easily investigate the role of the various building's features.

Keywords: Settlements · Numerical modelling · Masonry structures · Damage

1 Introduction

In many areas of the world, the occurrence of settlements due to human interventions and/or natural processes can harm existing historical structures. Challenges arise in the prediction of the distortions, displacements and damage that are likely to occur on such

Y. Endo and T. Hanazato (Eds.): SAHC 2023, RILEM Bookseries 46, pp. 232–244, 2024.
https://doi.org/10.1007/978-3-031-39450-8_19

buildings, since observations of full-scale structures are often limited or unavailable. Numerical simulations represent a widely adopted alternative to investigate the damage to historical buildings. Three-dimensional analyses may seem more appropriate to predict the response of the entire structure subjected to uneven settlement. However, they require increased computational resources and model complexity, and are thus associated with more uncertainties. Moreover, 3D models should include three-dimensional settlement configurations. The three-dimensional ground movements due to some settlement causes, such as tunnelling, excavation and mining activities, can be estimated with good accuracy [6]. However, for other sources of urban subsidence (e.g. groundwater changes, soil shrinkage, and organic soil oxidation), unpredictable ground profiles can arise [4, 6]. In such cases, the three-dimensional settlement patterns must be retrieved from in-situ survey measurements. Such measurements, however, are difficult to retrieve along all the building's walls in the case of terraced houses, as they share side walls. This is the case of many buildings in the Netherlands, for which bed-joint measurements are available only along the façades. In this context, two-dimensional models are often used as an alternative to investigate the building's response. In such 2D models, the effects of the house-to-house separation walls, i.e., the walls transversally connected to the façade, and of the floor system, may or may not be included. Thus, with a focus on historical unreinforced masonry buildings subjected to ground settlements, this study compares the results of six modelling approaches to select the most suitable and less costly in terms of computational resources and modelling burden. Among the selected modelling strategies, a novel 2D model is herein proposed to include the effects of the lateral house-to-house separation walls on the building's response.

2 Finite Element Models

In the last decades, the numerical models that simulate the response of structures undergoing ground movements have become increasingly detailed and accurate [11]. Thanks to the development and availability of computational resources, the modelling approach for structures subjected to settlements improved from elastic beams with equivalent axial and bending properties to complex 2D and 3D models, that include the non-linear behavior of the materials (e.g. in [7, 11, 20, 25–27, 29, 30]). The behavior of soil and of the soil-structure interaction in coupled analyses (i.e. models that include both the structure and the subsurface on which it rests), improved from an elastic continuum to non-linear constitutive laws that accurately predict the ground movements (e.g. in [8, 11, 24, 25]). However, coupled analyses involve the generation of complex meshes and high computational time and effort [11]. Therefore, a compromise is typically found with semi-coupled models. In semi-coupled analyses the ground movements are applied to an interface accounting for the soil and foundation stiffness [11, 26]. A similar approach involves applying the ground displacements to an interface accounting for the soil-foundation interaction, while the strip foundation system is explicitly included in the numerical model [11, 17, 27].

In this study, six modelling approaches inspired by the state of the art were selected and used for 2D and 3D analyses of a masonry structure subjected to subsidence-related settlements. Figure 1 summarizes the six selected models built with the finite element software Diana FEA 10.5:

a) 2D façade model (2DFA in Fig. 1a), a plane stress model of the building's façade [1, 5, 11];
b) 2D façade model (2DSF in Fig. 1b), a plane stress model with short lateral linear beam elements, with the width of one brick, that simulates the presence of transversal walls [15, 27];
c) 2D façade model (2DLF in Fig. 1c), a novel plane stress model with long lateral linear beam elements, whose cross-section width is wider than one brick, and non-linear springs placed at the sides of the strip foundation;
d) 3D façade model (3DFA in Fig. 1d), a three dimensional model of the building's façade;
e) 3D box model (3DBOX in Fig. 1e), a three dimensional model of the entire building, without floors and party walls (similar to [10]);
f) 3D full model (3DFULL in Fig. 1f), a three dimensional model of the entire building (similar to [7]).

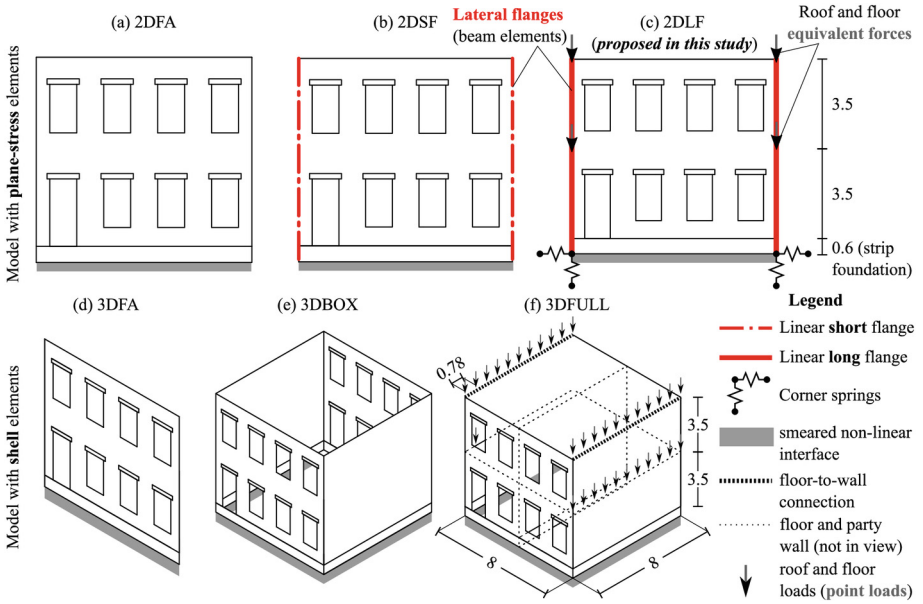

Fig. 1. The selected modelling approaches for the two-storey masonry building with a width of 8 m for both the façades and the transverse walls, a total height of 7 m and single-wythe (i.e. the width of one brick, equal to 100 mm) walls.: (a) 2D façade model (2DFA); (b) 2D façade with lateral linear short flanges (2DSF); (c) 2D façade with lateral linear long flanges (2DLF); (d) 3D façade model (3DFA); (e) 3D model (3DBOX); (f) 3D full model (3DFULL).

The models correspond to a two-storey masonry building with a width of 8 m, a total height of 7 m and single-wythe walls (i.e. the width of one brick, equal to 100 mm). Such a building idealizes typical old Dutch structures built before 1945 [13]. The models include the masonry strip foundation system below the walls, commonly observed in such old buildings, with a width and height of 500 and 600 mm respectively for which a soil-structure interaction interface is used [17]. All the models include openings underneath masonry lintels. 8-node quadratic elements with 3 × 3 Gaussian integration schemes were adopted for the façade, lintels, and foundation for both the 2D and 3D analyses. Six-noded line interface elements were used to model the soil-building interaction. A mesh size of 100 × 100 mm was used for the plane stress elements, and 100 mm for the beam elements. An orthotropic, smeared crack/shear/crush constitutive law was employed to explicitly simulate the cracking behavior of masonry (Engineering Masonry Model, [28]). The material properties of the selected fired clay brick masonry (Table 1) were retrieved from the Dutch Standard [21] and previous studies [14, 28], and were applied to both the façade and foundation.

Regarding the models that make use of lateral elements to simulate the effects of transverse walls (2DSF and 2DLF in Fig. 1b and c respectively), class-III Mindlin beam elements were placed on the two lateral sides of the façades, with the Young's modulus equal to 1/3rd of the one of masonry material (E_y in Table 1) the Poisson's ratio of 0.15 and the same mass density, following the approach implemented in [15, 27].

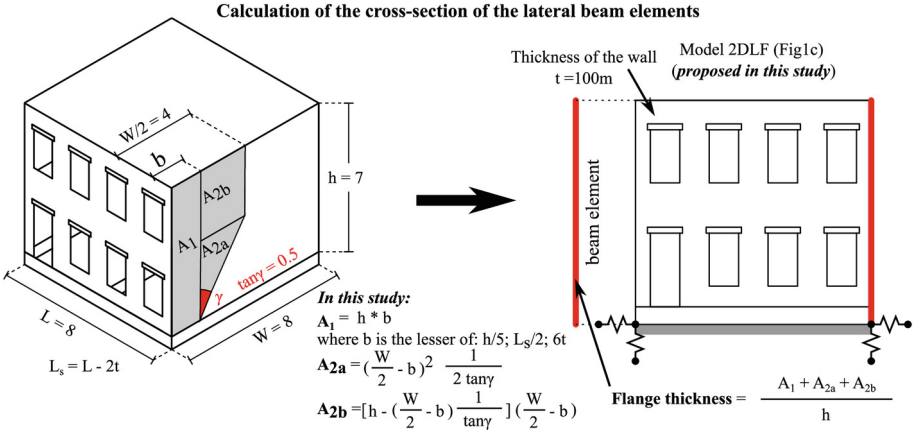

Fig. 2. Calculation of the cross-section of the lateral beam elements for the model 2DLF (Fig. 1c) as described in [22, 31]). Measures in meters.

Figure 2 illustrates how the thickness of the cross-section of the lateral elements was computed for the model 2DLF (Fig. 1c). This length corresponds to the sum of three contributions (A_1, A_{2a} and A_{2b} in Fig. 2), which provides the length of the cooperating flange (as described in [22, 31]). The first contribution (A_1 in Fig. 2) was computed by considering the minimum of the following transverse wall properties: a fifth of the wall height, half of the internal distance between party walls (L_s/2), or six times the wall thickness (t), as described in [31]. The obtained value (i.e. 0.6 m), is further supplemented

with the second and the third contributions (A_{2a} and A_{2b} in Fig. 2), which contributes to the normal compression given by the flange (as described in [22]). The total computed thickness for the lateral beam elements (Flange thickness in Fig. 2) is 2.35 m for the selected case.

In the case of 3DFULL, the timber floor and roof, commonly observed in the Dutch historical buildings, were modelled using elastic C24 class material for both the class-III Mindlin beam elements, representing the joists, and the orthotropic shell elements for the planks sheeting, calibrated according to [21]. The floor, roof and mid-party wall were disconnected from the front and back façades, thus, the weight of the roof and the floor system is transferred to the transverse walls employing point loads (Fig. 1f). In the proposed model 2DLF (Fig. 1c) the overburden of the floors acting on the lateral walls of the model 3DFULL (Fig. 1f) was simulated applying four equivalent forces, two per floor at each side of the façade (Fig. 1c). The four equivalent forces for the model 2DLF (Fig. 1c) were computed considering the portion of the floor and roof that loads the length of the cooperating flanges.

At the foundation, a zero-tension interface was modelled to consider the local soil-foundation interaction by means of boundary interface elements, connected to the bottom edge of the strip foundation [17].

Table 1. Material properties adopted in the FE models.

Material Properties	Symbol	Unit of measure	Value
Young's modulus vertical direction	E_y	[MPa]	5000
Young's modulus horizontal direction	E_x	[MPa]	2500
Shear modulus	G_{xy}	[MPa]	2000
Bed joint tensile strength	f_{ty}	[MPa]	0.10
Minimum head-joint strength	$f_{tx,min}$	[MPa]	0.15
Fracture energy in tension	$G_{ft,I}$	[N/mm]	0.01
Angle between stepped crack and bed-joint	α	[rad]	0.50
Compressive strength	f_c	[MPa]	8.50
Fracture energy in compression	G_c	[N/mm]	20.00
Friction angle	φ	[rad]	0.70
Cohesion	c	[MPa]	0.15
Fracture energy in shear	G_s	[N/mm]	0.10
Mass density	ρ	[Kg/m^3]	1708

The interface normal and tangential stiffnesses were computed using the equations reported by [9, 18, 19], on the basis of soil shear modulus G, Poisson's ratio ν, and foundation thickness (i.e. the base of the foundation in the direction transversal to the masonry façade). The selected soil properties simulate a clayey soil material, with the shear modulus equal to 10 MPa and the Poisson's ratio equal to 0.45. These stiffness

values were also adopted in the model 2DLF for the two corner springs (Fig. 1c) placed to support the weight of the lateral beam elements. Two types of asymmetric settlement deformations (i.e. hogging and sagging in Fig. 3) idealize the long-term (i.e. decades) ground displacements that develop during the service life of a historical structure. The settlement shapes, conformed to a Gaussian curve [23] described by Eq. (1), were applied at the base of the foundation.

$$S_v(x) = S_{v,max} \cdot \exp\left(-x^2/2x_i^2\right) \tag{1}$$

where $S_v(x)$ represents the vertical ground settlement, x_i is the distance from the symmetric axis of the curve to the point of inflection and $S_{v,max}$ is imposed to ensure the same intensity for all the profiles. The angular distortion β (i.e. the slope of the line joining two consecutive points in relation to a line joining the two points at the sides of each settlement profile [3]) was chosen to characterize the intensity of the settlement troughs. Accordingly, all the settlement profiles present the same angular distortion of 1/300. In the case of the 3D models, the settlement shapes were purposely assumed not to vary in the direction perpendicular to the plane of the façade, to exclude the effect of three-dimensional settlement variations. A two-phased load application procedure was adopted for all the models: the self-weight of the structure was applied in 10 steps to compute the initial stress-state, and then the settlement deformation was applied in 195 steps (with a load rate of 0.02 mm/step). The tabulated outputs of the analyses were then used to quantify the damage progression by means of a parameter (Ψ, proposed by [16]), based on the number of cracks, their length and opening. The corresponding damage severity was then categorized according to the system proposed by Burland et al. [3] (Table 2).

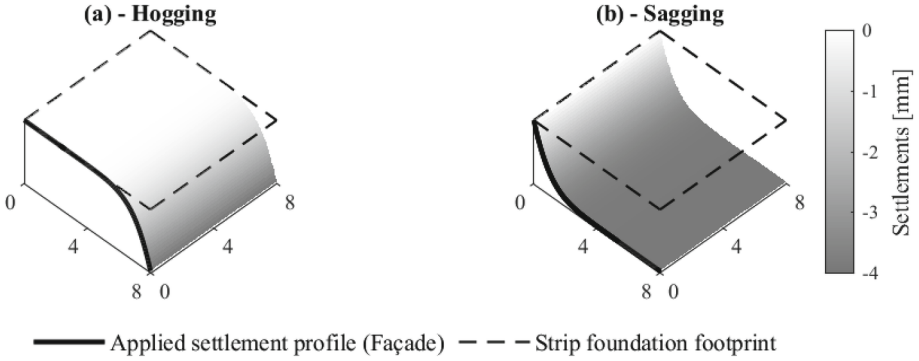

Fig. 3. Settlement profiles applied in the finite element models: (a) Hogging and (b) Sagging. In the 2D models, only the façade settlement (solid line in the figure) is applied below the interface elements (see Fig. 1), while for the 3D models the entire three-dimensional settlement pattern is applied. The settlement profile of the façade is conformed to a Gaussian distribution and it is characterized by an angular distortion equal to 1/300.

Table 2. Damage scale with the classification of visible damage and the corresponding discretization of the damage parameter in sub-levels (from [12, 16]).

Damage level	Degree of damage	Approximate crack width	Parameter of damage
DL0	No Damage	Imperceptible cracks	$\Psi < 1$
DL1	Negligible	up to 0.1 mm	$1 \leq \Psi < 1.5$
DL2	Very slight	up to 1 mm	$1.5 \leq \Psi < 2.5$
DL3	Slight	up to 5 mm	$2.5 \leq \Psi < 3.5$
DL4	Moderate	5 to 15 mm	$\Psi \geq 3.5$

3 Results

For each applied settlement profile, the vertical displacements at the façade's base (top edge of the foundation) were retrieved in the tabulated output. Thus, a distinction is introduced between the applied deformations at the interface level, identified with the prefix "applied", and the resulting façade displacements, identified with "retrieved". In Fig. 4a and b, the relationship between the applied angular distortion and the damage parameter Ψ is determined for both hogging and sagging. Particularly, the results of two façade models 2DFA (with plane stress elements) and 3DFA (with shell elements) overlap and show just minor differences (Fig. 4). Therefore, no major differences can be attributed to the type of finite elements (i.e. plane stress or shell elements). The three-dimensional models, 3DBOX and 3DFULL, are more vulnerable, exhibiting higher damage for the same angular distortion, than the façade models, 2DFA and 3DFA. While the model with a short lateral flange, 2DSF, shows results comparable with the other 2D cases, the proposed model with a long lateral flange (i.e., 2DLF) is able to better depict the vulnerable behavior of the 3D full-scale cases.

Interestingly, smaller differences between the behavior of the models are observed when the retrieved angular distortion was plotted against the damage parameter (Fig. 4c and d), meaning that the observed deformation is mainly correlated to the shape and the stiffness of the façade itself. Regarding the difference between the applied and the retrieved values of the angular distortion, shown in Fig. 4e and f for hogging and sagging respectively, the plotted lines are compared with a dash-dotted line that represents the condition for which applied and retrieved values would be equal (Fig. 4). The results of the models 2DLF, 3DBOX and 3DFULL progressively get closer to the theoretical line. This observation suggests that the 2DLF model better accommodates the imposed deformation with the damage progression. On the contrary, the same behavior is not observed for the two façade models, 2DFA and 3DFA, and it's less clear for the model with short lateral elements, 2DSF. A comparison of the exhibited crack patterns of all models (i.e. position and direction of the cracks) is proposed in Fig. 5 for an imposed angular distortion of 2 ‰ (or 1/500) for both hogging and sagging deformations.

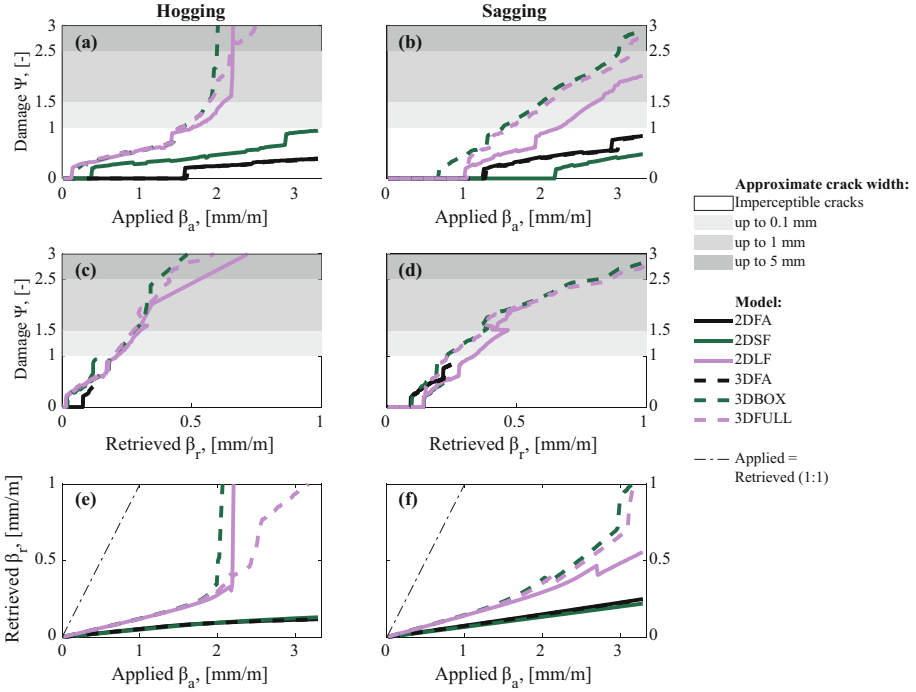

Fig. 4. Angular distortion against the resulting damage patterns for all the FE models for both hogging and sagging. The approximate crack width ranges corresponding to damage parameter Ψ (Table 2) are shown. The results of the models 2DFA and 3DFA overlap in all the plots.

The façade models, 2DFA and 3DFA, and the model with short lateral elements, 2DSF, underestimate the damage (in terms of Ψ), both in hogging and sagging when compared with 3DFULL. The 3DBOX model, in which the effects of the party wall and floors are not included, overestimates the damage severity in hogging, while, on the contrary, it is less vulnerable to sagging. A better agreement of the results is observed when the reference case (3DFULL) is compared with the 2DLF model. Particularly, not only the damage severity (in terms of Ψ), but also the crack patterns are similar.

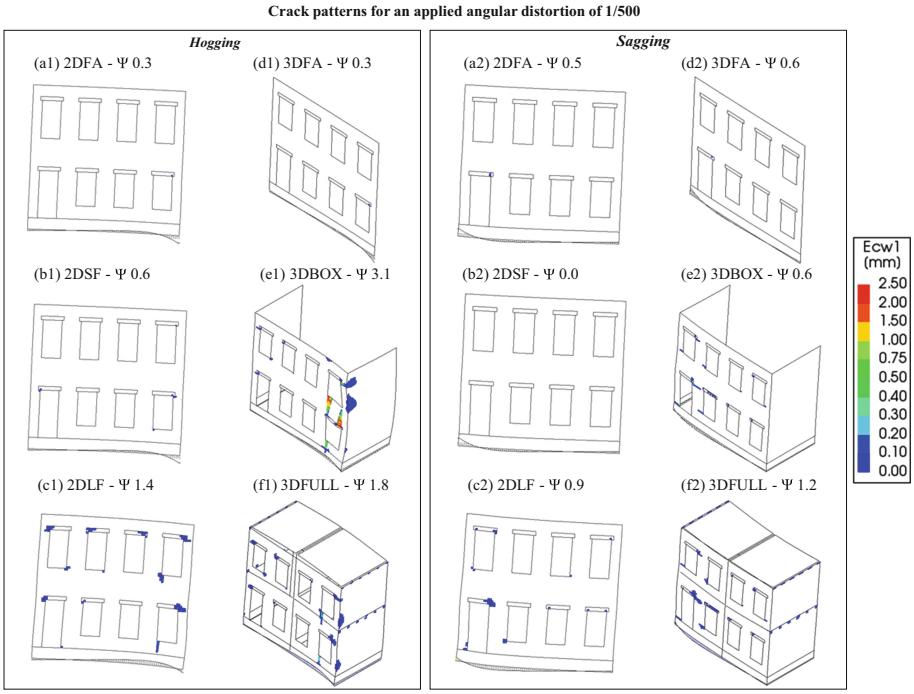

Fig. 5. Resulting crack patterns for all the FE models at an applied angular distortion of 1/500. The crack width is shown. The damage parameter Ψ is reported for every model. (e1), (f1), (e2) and (f2) depict half the model. Magnification factor of the deformation equals to 300.

The comparison between the normal interface stresses of all the numerical models is proposed in Fig. 6, for an applied angular distortion of 2 ‰ (or 1/500). For the hogging deformation, a good agreement with the reference case is observed in the case of the 2DLF and 3DBOX models. Particularly, the stresses represent a compression of the entire interface, while for the other models, 2DFA, 2DSF and 3DFA part of the interface shows the formation of a gap. Similarly, in the case of sagging, the 2DLF, 3DBOX and 3DFULL are in good agreement. The differences between the interface stresses may be attributed to the influence of the weight and stiffness of lateral walls. The presence of a wider transversal wall (with additional weight) and the corner springs (additional stiffness) in the 2DLF model allows for a better representation of the three dimensional effects. A comparison of the models' features (type of elements, number of elements and nodes) and their performance in terms of computational time is shown in Table 3. For this purpose, two additional analyses, making use of the structural symmetry, were carried out for the full-scale 3D models, labelled as 3DBOX-Half and 3DFULL-Half (Table 3). The analysis time of each model for the hogging profile (Fig. 3a) was normalized to the one of the 2DLF model. The 3D models are 9 to 28 times slower in terms of computational time due to the high number of elements and nodes, when compared with 2D analyses. These estimates do not include generating the models or setting up the analyses but comprise only the CPU time.

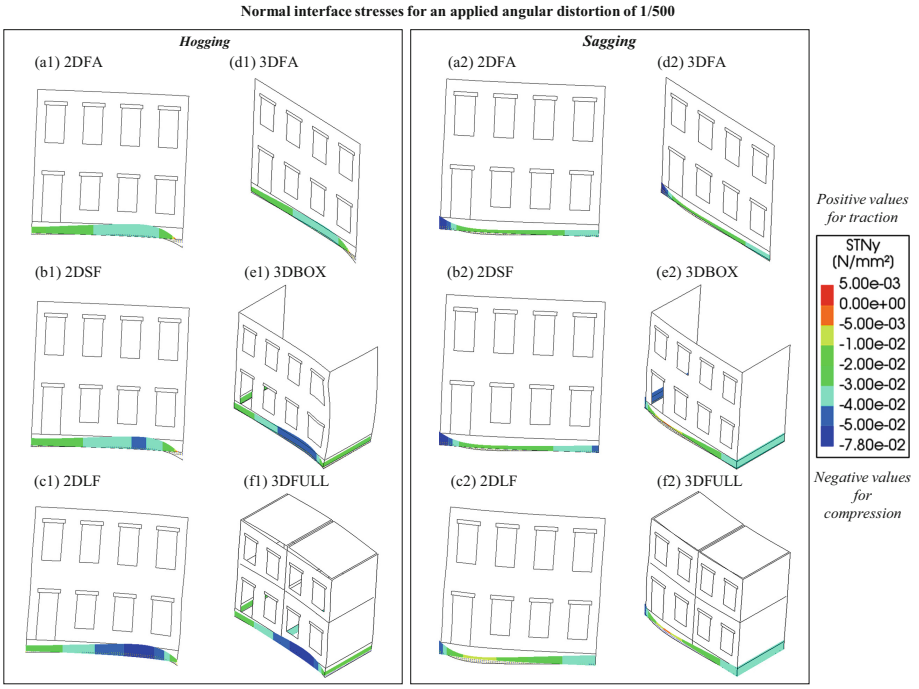

Fig. 6. Normal interface stresses for hogging and sagging, with applied angular distortion of 1/500. Positive values represent tension, negative ones, compression. (e1), (f1), (e2) and (f2) depict half the model. Magnification factor of the deformation equals 300.

Table 3. A comparison of all the selected modelling strategy features. The values of the proposed modelling approach 2DLF (Fig. 1c) are shaded in the table.

Model	Type of Elements	Elements	Nodes	Analysis Time [hh:mm:ss]	Normalized Analysis Time
2DFA	2D Plane Stress	4570	14414	0:05:59	0.23
2DSF	2D Plane Stress	4722	14414	0:07:57	0.31
2DLF	2D Plane Stress	4724	14414	0:25:47	1.00
3DFA	3D Shell	4650	14638	0:30:39	1.19
3DBOX	3D Shell	21620	66088	8:10:33	10.03
3DFULL	3D Shell	41580	121944	12:04:26	28.10
3DBOX-Half	3D Shell	10810	33198	3:50:18	8.93
3DFULL-Half	3D Shell	61436	20895	6:17:41	14.65

4 Discussion

This study focused on the effect of settlement shapes that do not present variations along the direction perpendicular to the plane of the façade. However, in many real cases the settlements may present 3D patterns. Thus, a 2D analysis may not be able to accurately depict the structural response. Moreover, 2D analyses do not include out-of-plane effects of the walls. In this study, out-of-plane displacements in the 3D models were observed to reach a maximum of 1.7 mm, and are thus considered negligible. Moreover, further improvements may include the effect given by separation walls with openings or the lateral confinement by the floor system, for instance, by means of discrete lateral springs.

In this work, the horizontal ground movements were purposively neglected. Such horizontal components of the ground deformations were observed to be significant in the case of tunnelling, mining or excavation works [2], whereas this study focuses on the settlements due to a combination of subsidence drivers (e.g. organic soil oxidation, groundwater lowering, soil shrinkage) in urban areas. Due to the limited empirical knowledge in the state of the art on the transmission of the horizontal displacements and stresses between the soil and the foundation due to subsidence-related settlements, in this study a smooth interface was used for all the models.

5 Conclusion

It was observed that the models including only the façade of the building, 2DFA and 3DFA exhibit lower values of damage for a given applied angular distortion when compared with the full-scale three-dimensional ones, 3DBOX and 3DFULL. Among the 2D models that include the effect of house-to-house separation walls by means of lateral linear elements, the results of the model with long flanges, labelled as 2DLF, in terms of deformations, damage severity, and crack patterns, are in good agreement with the ones of the full-scale structure with floors and party wall, 3DFULL. This observation suggests that the proposed modelling strategy, 2DLF, depicts with good accuracy the behavior of the entire structure subjected to settlement. In addition, the resulting stresses at the interface, which account for the stiffness and the mass of the transversal walls, are also in good agreement with the 3DFULL model. Due to the different stresses at the interface, the prescribed settlements result in lower deformation in the case of the models that do not include the effect of the lateral walls, thus, less damage.

The proposed modelling strategy, 2DLF, was observed to be less costly in terms of time and computational resources than the full-scale three-dimensional analyses. The results of this study provide a background in the choice of the most suitable modelling strategy for masonry structures affected by ground movements.

Acknowledgments. The research presented here is part of the NWA project Living on Soft Soils: Subsidence and Society (grantnr.: NWA.1160.18.259).

References

1. Bejarano-Urrego, L., et al.: Numerical analysis of settlement-induced damage to a masonry church nave wall. In: Aguilar, R., Torrealva, D., Moreira, S., Pando, M.A., Ramos, L.F. (eds.) Structural Analysis of Historical Constructions. RILEM Bookseries, vol. 18, pp. 853–861 (2019). Springer, Cham. https://doi.org/10.1007/978-3-319-99441-3_92
2. Boscardin, M.D., Cording, E.J.: Building response to excavation-induced settlement. J. Geotech. Eng.-Asce. **115**, 1–21 (1989)
3. Burland, J.B., Wroth, C.: Settlement of buildings and associated damage (1975)
4. Charles, J.A., Skinner, H.D.: Settlement and tilt of low-rise buildings. Proc. Inst. Civil Eng.-Geotech. Eng. **157**, 65–75 (2004)
5. Drougkas, A., Verstrynge, E., Szeker, P., et al.: Numerical modeling of a church nave wall subjected to differential settlements: soil-structure interaction, time-dependence and sensitivity analysis. Int. J. Archit. Heritage. **14**, 1221–1238 (2020)
6. Drougkas, A., Verstrynge, E., Van Balen, K., et al.: Country-scale InSAR monitoring for settlement and uplift damage calculation in architectural heritage structures. Struct. Health Monit. Int. J. **20**, 2317–2336 (2020)
7. Ferlisi, S., Nicodemo, G., Peduto, D.: Numerical analysis of the behaviour of masonry buildings undergoing differential settlements (2019)
8. Franzius, J.N.: Behaviour of buildings due to tunnel induced subsidence: Imperial College London (University of London) (2004)
9. Gazetas, G.: Foundation vibrations. In: Fang, H.Y. (eds.) Foundation Engineering Handbook. Springer, Boston (1991). https://doi.org/10.1007/978-1-4757-5271-7_15
10. Giardina, G., Rots, J., Hendriks, M.: Modelling of settlement induced building damage. TU Delft, Delft. 2013
11. Giardina, G., Van de Graaf, A.V., Hendriks, M.A.N., et al.: Numerical analysis of a masonry facade subject to tunnelling-induced settlements. Eng. Struct. **54**, 234–247 (2013)
12. Grünthal, G.: European macroseismic scale 1998. European Seismological Commission (ESC) (1998)
13. Jafari, S.: Material characterisation of existing masonry: A strategy to determine strength, stiffness and toughness properties for structural analysis. Delft University of Technology: TU Delft Applied Mechanics https://repositorytudelf.tnl. Doctoral thesis (2021)
14. Korswagen Eguren, P.A., Longo, M., Meulman, E., et al.: Damage sensitivity of Groningen masonry structures–Experimental and computational studies: stream 1 (2017)
15. Korswagen, P.A., Longo, M., Meulman, E., et al.: Experimental and computational study of the influence of pre-damage patterns in unreinforced masonry crack propagation due to induced, repeated earthquakes. In: 13th North American Masonry Conference: TMS, p. 1628–45 (2019)
16. Korswagen, P.A., Longo, M., Meulman, E., Rots, J.G.: Crack initiation and propagation in unreinforced masonry specimens subjected to repeated in-plane loading during light damage. Bull. Earthq. Eng. **17**(8), 4651–4687 (2019). https://doi.org/10.1007/s10518-018-00553-5
17. Longo, M., Sousamli, M., Korswagen, P.A., et al.: Sub-structure-based "three-tiered" finite element approach to soil-masonry-wall interaction for light seismic motion. Eng. Struct. **245**, 112847 (2021)
18. Mylonakis, G., Nikolaou, S., Gazetas, G.: Footings under seismic loading: Analysis and design issues with emphasis on bridge foundations. Soil Dyn. Earthq. Eng. **26**, 824–853 (2006)
19. NEHRP. NIST GCR 12-917-21 Soil–structure interaction for building structures. Gaithersburg: National Institute of Standards and Technology, US Department of Commerce (2012)
20. Netzel, H.D.: Building response due to ground movements (2009)

21. NPR9998:2020en. Assessment of structural safety of buildings in case of erection, reconstruction and disapproval - Induced earthquakes - Basis of design, actions and resistances (2021)
22. NPR 9096-1-1:2012 nl. Steenconstructies - Eenvoudige ontwerpregels, gebaseerd op NEN-EN 1996-1-1+C1 (Masonry structures - Simple design rules, based on NEN-EN 1996–1–1+C1) (2012)
23. Peck, R.B.: Deep excavations and tunneling in soft ground. In: Proceedings of 7th ICSMFE, vol. 1969, pp. 225-90 (1969)
24. Peduto, D., Prosperi, A., Nicodemo, G., et al.: District-scale numerical analysis of settlements related to groundwater lowering in variable soil conditions. Can. Geotech. J. **99**, 1–16 (2022)
25. Potts, D.M., Addenbrooke, T.I.: A structure's influence on tunnelling-induced ground movements. Proc. Inst. Civil Eng.-Geotech. Eng. **125**, 109–125 (1997)
26. Rots, J.: Computational modelling of cracking and settlement damage in masonry structures. In: Proceedings of 12th International Brick/Block Masonry Conference, pp. 2171–2187 (2001)
27. Rots, J.G., Korswagen, P.A., Longo, M.: Computational modelling checks of masonry building damage due to deep subsidence. Delft University of Technology (2021)
28. Schreppers, G., Garofano, A., Messali, F., et al.: DIANA validation report for masonry modelling. DIANA FEA report. (2016)
29. Son, M., Cording, E.J.: Estimation of building damage due to excavation-induced ground movements. J. Geotech. Geoenvironmental Eng. **131**, 162–177 (2005)
30. Son, M., Cording, E.J.: Evaluation of building stiffness for building response analysis to excavation-induced ground movements. Journal of Geotech. Geoenvironmental Eng. **133**, 995–1002 (2007)
31. Standard B. Eurocode 6—Design of masonry structures—. British Standard Institution London (2005)